

Observation of Ξ^- hyperon transverse polarization in $\psi(3686) \rightarrow \Xi^-\bar{\Xi}^+$

- M. Ablikim¹, M. N. Achasov^{10,b}, P. Adlarson⁶⁸, M. Albrecht⁴, R. Aliberti²⁸, A. Amoroso^{67A,67C}, M. R. An³², Q. An^{64,50}, X. H. Bai⁵⁸, Y. Bai⁴⁹, O. Bakina²⁹, R. Baldini Ferroli^{23A}, I. Balossino^{24A}, Y. Ban^{39,g}, V. Batozskaya^{1,37}, D. Becker²⁸, K. Begzsuren²⁶, N. Berger²⁸, M. Bertani^{23A}, D. Bettoni^{24A}, F. Bianchi^{67A,67C}, J. Bloms⁶¹, A. Bortone^{67A,67C}, I. Boyko²⁹, R. A. Briere⁵, A. Brueggemann⁶¹, H. Cai⁶⁹, X. Cai^{1,50}, A. Calcaterra^{23A}, G. F. Cao^{1,55}, N. Cao^{1,55}, S. A. Cetin^{54A}, J. F. Chang^{1,50}, W. L. Chang^{1,55}, G. Chelkov^{29,a}, C. Chen³⁶, G. Chen¹, H. S. Chen^{1,55}, M. L. Chen^{1,50}, S. J. Chen³⁵, T. Chen¹, X. R. Chen^{25,55}, X. T. Chen¹, Y. B. Chen^{1,50}, Z. J. Chen^{20,h}, W. S. Cheng^{67C}, X. Chu³⁶, G. Cibinetto^{24A}, F. Cossio^{67C}, J. J. Cui⁴², H. L. Dai^{1,50}, J. P. Dai⁷¹, A. Dbeysi¹⁴, R. E. de Boer⁴, D. Dedovich²⁹, Z. Y. Deng¹, A. Denig²⁸, I. Denysenko²⁹, M. Destefanis^{67A,67C}, F. De Mori^{67A,67C}, Y. Ding³³, J. Dong^{1,50}, L. Y. Dong^{1,55}, M. Y. Dong^{1,50,55}, X. Dong⁶⁹, S. X. Du⁷³, P. Egorov^{29,a}, Y. L. Fan⁶⁹, J. Fang^{1,50}, S. S. Fang^{1,55}, W. X. Fang¹, Y. Fang¹, R. Farinelli^{24A}, L. Fava^{67B,67C}, F. Feldbauer⁴, G. Felici^{23A}, C. Q. Feng^{64,50}, J. H. Feng⁵¹, K. Fischer⁶², M. Fritsch⁴, C. Fritsch⁶¹, C. D. Fu¹, H. Gao⁵⁵, Y. N. Gao^{39,g}, Yang Gao^{64,50}, S. Garbolino^{67C}, I. Garzia^{24A,24B}, P. T. Ge⁶⁹, C. Geng⁵¹, E. M. Gersabeck⁵⁹, A. Gilman⁶², K. Goetzen¹¹, L. Gong³³, W. X. Gong^{1,50}, W. Gradi²⁸, M. Greco^{67A,67C}, M. H. Gu^{1,50}, C. Y. Guan^{1,55}, A. Q. Guo^{25,55}, L. B. Guo³⁴, R. P. Guo⁴¹, Y. P. Guo^{9,f}, A. Guskov^{29,a}, T. T. Han⁴², W. Y. Han³², X. Q. Hao¹⁵, F. A. Harris⁵⁷, K. K. He⁴⁷, K. L. He^{1,55}, F. H. Heinsius⁴, C. H. Heinz²⁸, Y. K. Heng^{1,50,55}, C. Herold⁵², M. Himmelreich^{11,d}, T. Holtmann⁴, G. Y. Hou^{1,55}, Y. R. Hou⁵⁵, Z. L. Hou¹, H. M. Hu^{1,55}, J. F. Hu^{48,i}, T. Hu^{1,50,55}, Y. Hu¹, G. S. Huang^{64,50}, K. X. Huang⁵¹, L. Q. Huang^{25,55}, L. Q. Huang⁶⁵, X. T. Huang⁴², Y. P. Huang¹, Z. Huang^{39,g}, T. Hussain⁶⁶, N. Hüskens^{22,28}, W. Imoehl²², M. Irshad^{64,50}, J. Jackson²², S. Jaeger⁴, S. Janchiv²⁶, Q. Ji¹, Q. P. Ji¹⁵, X. B. Ji^{1,55}, X. L. Ji^{1,50}, Y. Y. Ji⁴², Z. K. Jia^{64,50}, H. B. Jiang⁴², S. S. Jiang³², X. S. Jiang^{1,50,55}, Y. Jiang⁵⁵, J. B. Jiao⁴², Z. Jiao¹⁸, S. Jin³⁵, Y. Jin⁵⁸, M. Q. Jing^{1,55}, T. Johansson⁶⁸, N. Kalantar-Nayestanaki⁵⁶, X. S. Kang³³, R. Kappert⁵⁶, M. Kavatsyuk⁵⁶, B. C. Ke⁷³, I. K. Keshk⁴, A. Khoukaz⁶¹, P. Kiese²⁸, R. Kiuchi¹, R. Kliemt¹¹, L. Koch³⁰, O. B. Kolcu^{54A}, B. Kopf⁴, M. Kuemmel⁴, M. Kuessner⁴, A. Kupsc^{37,68}, W. Kühn³⁰, J. J. Lane⁵⁹, J. S. Lange³⁰, P. Larin¹⁴, A. Lavania²¹, L. Lavezzi^{67A,67C}, Z. H. Lei^{64,50}, H. Leithoff²⁸, M. Lellmann²⁸, T. Lenz²⁸, C. Li³⁶, C. Li⁴⁰, C. H. Li³², Cheng Li^{64,50}, D. M. Li⁷³, F. Li^{1,50}, G. Li¹, H. Li⁴⁴, H. Li^{64,50}, H. B. Li^{1,55}, H. J. Li¹⁵, H. N. Li^{48,i}, J. Q. Li⁴, J. S. Li⁵¹, J. W. Li⁴², Ke Li¹, L. J Li¹, L. K. Li¹, Lei Li³, M. H. Li³⁶, P. R. Li^{31,j,k}, S. X. Li⁹, S. Y. Li⁵³, T. Li⁴², W. D. Li^{1,55}, W. G. Li¹, X. H. Li^{64,50}, X. L. Li⁴², Xiaoyu Li^{1,55}, Z. Y. Li⁵¹, H. Liang^{1,55}, H. Liang²⁷, H. Liang^{64,50}, Y. F. Liang⁴⁶, Y. T. Liang^{25,55}, G. R. Liao¹², L. Z. Liao⁴², J. Libby²¹, A. Limphirat⁵², C. X. Lin⁵¹, D. X. Lin^{25,55}, T. Lin¹, B. J. Liu¹, C. X. Liu¹, D. Liu^{14,64}, F. H. Liu⁴⁵, Fang Liu¹, Feng Liu⁶, G. M. Liu^{48,i}, H. Liu^{31,j,k}, H. M. Liu^{1,55}, Huanhuan Liu¹, Huihui Liu¹⁶, J. B. Liu^{64,50}, J. L. Liu⁶⁵, J. Y. Liu^{1,55}, K. Liu¹, K. Y. Liu³³, Ke Liu¹⁷, L. Liu^{64,50}, M. H. Liu^{9,f}, P. L. Liu¹, Q. Liu⁵⁵, S. B. Liu^{64,50}, T. Liu^{9,f}, W. K. Liu³⁶, W. M. Liu^{64,50}, X. Liu^{31,j,k}, Y. Liu^{31,j,k}, Y. B. Liu³⁶, Z. A. Liu^{1,50,55}, Z. Q. Liu⁴², X. C. Lou^{1,50,55}, F. X. Lu⁵¹, H. J. Lu¹⁸, J. G. Lu^{1,50}, X. L. Lu¹, Y. Lu¹, Y. P. Lu^{1,50}, Z. H. Lu¹, C. L. Luo³⁴, M. X. Luo⁷², T. Luo^{9,f}, X. L. Luo^{1,50}, X. R. Lyu⁵⁵, Y. F. Lyu³⁶, F. C. Ma³³, H. L. Ma¹, L. L. Ma⁴², M. M. Ma^{1,55}, Q. M. Ma¹, R. Q. Ma^{1,55}, R. T. Ma⁵⁵, X. Y. Ma^{1,50}, Y. Ma^{39,g}, F. E. Maas¹⁴, M. Maggiora^{67A,67C}, S. Maldaner⁴, S. Malde⁶², Q. A. Malik⁶⁶, A. Mangoni^{23B}, Y. J. Mao^{39,g}, Z. P. Mao¹, S. Marcello^{67A,67C}, Z. X. Meng⁵⁸, J. G. Messchendorp^{56,11}, G. Mezzadri^{24A}, H. Miao¹, T. J. Min³⁵, R. E. Mitchell²², X. H. Mo^{1,50,55}, N. Yu. Muchnoi^{10,b}, H. Muramatsu⁶⁰, Y. Nefedov²⁹, F. Nerling^{11,d}, I. B. Nikolaev^{10,b}, Z. Ning^{1,50}, S. Nisar^{8,l}, Y. Niu⁴², S. L. Olsen⁵⁵, Q. Ouyang^{1,50,55}, S. Pacetti^{23B,23C}, X. Pan^{9,f}, Y. Pan⁵⁹, A. Pathak¹, A. Pathak²⁷, M. Pelizaeus⁴, H. P. Peng^{64,50}, K. Peters^{11,d}, J. Pettersson⁶⁸, J. L. Ping³⁴, R. G. Ping^{1,55}, S. Plura²⁸, S. Pogodin²⁹, R. Poling⁶⁰, V. Prasad^{64,50}, F. Z. Qi¹, H. Qi^{64,50}, H. R. Qi⁵³, M. Qi³⁵, T. Y. Qi^{9,f}, S. Qian^{1,50}, W. B. Qian⁵⁵, Z. Qian⁵¹, C. F. Qiao⁵⁵, J. J. Qin⁶⁵, L. Q. Qin¹², X. P. Qin^{9,f}, X. S. Qin⁴², Z. H. Qin^{1,50}, J. F. Qiu¹, S. Q. Qu³⁶, S. Q. Qu⁵³, K. H. Rashid⁶⁶, C. F. Redmer²⁸, K. J. Ren³², A. Rivetti^{67C}, V. Rodin⁵⁶, M. Roloff^{67C}, G. Rong^{1,55}, Ch. Rosner¹⁴, S. N. Ruan³⁶, H. S. Sang⁶⁴, A. Sarantsev^{29,c}, Y. Schelhaas²⁸, C. Schnier⁴, K. Schoenning⁶⁸, M. Scodeggio^{24A,24B}, K. Y. Shan^{9,f}, W. Shan¹⁹, X. Y. Shan^{64,50}, J. F. Shangguan⁴⁷, L. G. Shao^{1,55}, M. Shao^{64,50}, C. P. Shen^{9,f}, H. F. Shen^{1,55}, X. Y. Shen^{1,55}, B.-A. Shi⁵⁵, H. C. Shi^{64,50}, J. Y. Shi¹, R. S. Shi^{1,55}, X. Shi^{1,50}, X. D. Shi^{64,50}, J. J. Song¹⁵, W. M. Song^{27,1}, Y. X. Song^{39,g}, S. Sosio^{67A,67C}, S. Spataro^{67A,67C}, F. Stieler²⁸, K. X. Su⁶⁹, P. P. Su⁴⁷, Y.-J. Su⁵⁵, G. X. Sun¹, H. Sun⁵⁵, H. K. Sun¹, J. F. Sun¹⁵, L. Sun⁶⁹, S. S. Sun^{1,55}, T. Sun^{1,55}, W. Y. Sun²⁷, X. Sun^{20,h}, Y. J. Sun^{64,50}, Y. Z. Sun¹, Z. T. Sun⁴², Y. H. Tan⁶⁹, Y. X. Tan^{64,50}, C. J. Tang⁴⁶, G. Y. Tang¹, J. Tang⁵¹, L. Y Tao⁶⁵, Q. T. Tao^{20,h}, J. X. Teng^{64,50}, V. Thoren⁶⁸, W. H. Tian⁴⁴, Y. Tian^{25,55}, I. Uman^{54B}, B. Wang¹, B. L. Wang⁵⁵, D. Y. Wang^{39,g}, F. Wang⁶⁵, H. J. Wang^{31,j,k}, H. P. Wang^{1,55}, K. Wang^{1,50}, L. L. Wang¹, M. Wang⁴², M. Z. Wang^{39,g}, Meng Wang^{1,55}, S. Wang^{9,f}, T. Wang^{9,f}, T. J. Wang³⁶, W. Wang⁵¹, W. H. Wang⁶⁹, W. P. Wang^{64,50}, X. Wang^{39,g}, X. F. Wang^{31,j,k}, X. L. Wang^{9,f}, Y. D. Wang³⁸, Y. F. Wang^{1,50,55}, Y. H. Wang⁴⁰, Y. Q. Wang¹, Ying Wang⁵¹, Z. Wang^{1,50}, Z. Y. Wang^{1,55}, Ziyi Wang⁵⁵, D. H. Wei¹², F. Weidner⁶¹, S. P. Wen¹, D. J. White⁵⁹, U. Wiedner⁴, G. Wilkinson⁶², M. Wolke⁶⁸, L. Wollenberg⁴, J. F. Wu^{1,55}, L. H. Wu¹, L. J. Wu^{1,55}, X. Wu^{9,f}, X. H. Wu²⁷, Y. Wu⁶⁴, Z. Wu^{1,50}, L. Xia^{64,50}, T. Xiang^{39,g}, D. Xiao^{31,j,k}, H. Xiao^{9,f}, S. Y. Xiao¹, Y. L. Xiao^{9,f}, Z. J. Xiao³⁴, X. H. Xie^{39,g}, Y. Xie⁴², Y. G. Xie^{1,50}, Y. H. Xie⁶, Z. P. Xie^{64,50}, T. Y. Xing^{1,55}, C. F. Xu¹, C. J. Xu⁵¹, G. F. Xu¹, H. Y. Xu⁵⁸, Q. J. Xu¹³, S. Y. Xu⁶³, X. P. Xu⁴⁷, Y. C. Xu⁵⁵, F. Yan^{9,f}, L. Yan^{9,f}, W. B. Yan^{64,50}, W. C. Yan⁷³, H. J. Yang^{43,e}, H. L. Yang²⁷, H. X. Yang¹, L. Yang⁴⁴, S. L. Yang⁵⁵, Tao Yang¹, Y. X. Yang^{1,55}, Yifan Yang^{1,55}, M. Ye^{1,50}, M. H. Ye⁷, J. H. Yin¹, Z. Y. You⁵¹, B. X. Yu^{1,50,55}, C. X. Yu³⁶, G. Yu^{1,55}, T. Yu⁶⁵, C. Z. Yuan^{1,55}, L. Yuan², S. C. Yuan¹, X. Q. Yuan¹, Y. Yuan^{1,55}, Z. Y. Yuan⁵¹, C. X. Yue³², A. A. Zafar⁶⁶, F. R. Zeng⁴², X. Zeng Zeng⁶, Y. Zeng^{20,h}, Y. H. Zhan⁵¹, A. Q. Zhang¹, B. L. Zhang¹, B. X. Zhang¹, D. H. Zhang³⁶, G. Y. Zhang¹⁵, H. Zhang⁶⁴, H. H. Zhang²⁷, H. H. Zhang⁵¹, H. Y. Zhang^{1,50}, J. L. Zhang⁷⁰, J. Q. Zhang³⁴, J. W. Zhang^{1,50,55}, J. X. Zhang^{31,j,k}, J. Y. Zhang¹, J. Z. Zhang^{1,55}, Jianyu Zhang^{1,55}, Jiawei Zhang^{1,55}, L. M. Zhang⁵³, L. Q. Zhang⁵¹, Lei Zhang³⁵, P. Zhang¹, Q. Y. Zhang^{32,73}, Shulei Zhang^{20,h}, X. D. Zhang³⁸, X. M. Zhang¹, X. Y. Zhang⁴⁷, X. Y. Zhang⁴², Y. Zhang⁶², Y. T. Zhang⁷³, Y. H. Zhang^{1,50}, Yan Zhang^{64,50}, Yao Zhang¹, Z. H. Zhang¹, Z. Y. Zhang⁶⁹, Z. Y. Zhang³⁶, G. Zhao¹, J. Zhao³², J. Y. Zhao^{1,55}, J. Z. Zhao^{1,50}, Lei Zhao^{64,50}, Ling Zhao¹, M. G. Zhao³⁶, Q. Zhao¹, S. J. Zhao⁷³, Y. B. Zhao^{1,50}, Y. X. Zhao^{25,55}, Z. G. Zhao^{64,50}, A. Zhemchugov^{29,a}, B. Zheng⁶⁵, J. P. Zheng^{1,50}, Y. H. Zheng⁵⁵, B. Zhong³⁴, C. Zhong⁶⁵, X. Zhong⁵¹, H. Zhou⁴², L. P. Zhou^{1,55}, X. Zhou⁶⁹, X. K. Zhou⁵⁵, X. R. Zhou^{64,50}, X. Y. Zhou³², Y. Z. Zhou^{9,f}, J. Zhu³⁶, K. Zhu¹, K. J. Zhu^{1,50,55}, L. X. Zhu⁵⁵, S. H. Zhu⁶³, T. J. Zhu⁷⁰, W. J. Zhu^{9,f}, Y. C. Zhu^{64,50}, Z. A. Zhu^{1,55}, B. S. Zou¹, J. H. Zou¹

(BESIII Collaboration)

¹ Institute of High Energy Physics, Beijing 100049, People's Republic of China

- ² Beihang University, Beijing 100191, People's Republic of China
³ Beijing Institute of Petrochemical Technology, Beijing 102617, People's Republic of China
⁴ Bochum Ruhr-University, D-44780 Bochum, Germany
⁵ Carnegie Mellon University, Pittsburgh, Pennsylvania 15213, USA
⁶ Central China Normal University, Wuhan 430079, People's Republic of China
⁷ China Center of Advanced Science and Technology, Beijing 100190, People's Republic of China
⁸ COMSATS University Islamabad, Lahore Campus, Defence Road, Off Raiwind Road, 54000 Lahore, Pakistan
⁹ Fudan University, Shanghai 200433, People's Republic of China
¹⁰ G.I. Budker Institute of Nuclear Physics SB RAS (BINP), Novosibirsk 630090, Russia
¹¹ GSI Helmholtzcentre for Heavy Ion Research GmbH, D-64291 Darmstadt, Germany
¹² Guangxi Normal University, Guilin 541004, People's Republic of China
¹³ Hangzhou Normal University, Hangzhou 310036, People's Republic of China
¹⁴ Helmholtz Institute Mainz, Staudinger Weg 18, D-55099 Mainz, Germany
¹⁵ Henan Normal University, Xinxiang 453007, People's Republic of China
¹⁶ Henan University of Science and Technology, Luoyang 471003, People's Republic of China
¹⁷ Henan University of Technology, Zhengzhou 450001, People's Republic of China
¹⁸ Huangshan College, Huangshan 245000, People's Republic of China
¹⁹ Hunan Normal University, Changsha 410081, People's Republic of China
²⁰ Hunan University, Changsha 410082, People's Republic of China
²¹ Indian Institute of Technology Madras, Chennai 600036, India
²² Indiana University, Bloomington, Indiana 47405, USA
²³ INFN Laboratori Nazionali di Frascati, (A)INFN Laboratori Nazionali di Frascati, I-00044, Frascati, Italy; (B)INFN Sezione di Perugia, I-06100, Perugia, Italy; (C)University of Perugia, I-06100, Perugia, Italy
²⁴ INFN Sezione di Ferrara, (A)INFN Sezione di Ferrara, I-44122, Ferrara, Italy; (B)University of Ferrara, I-44122, Ferrara, Italy
²⁵ Institute of Modern Physics, Lanzhou 730000, People's Republic of China
²⁶ Institute of Physics and Technology, Peace Ave. 54B, Ulaanbaatar 13330, Mongolia
²⁷ Jilin University, Changchun 130012, People's Republic of China
²⁸ Johannes Gutenberg University of Mainz, Johann-Joachim-Becher-Weg 45, D-55099 Mainz, Germany
²⁹ Joint Institute for Nuclear Research, 141980 Dubna, Moscow region, Russia
³⁰ Justus-Liebig-Universitaet Giessen, II. Physikalisches Institut, Heinrich-Buff-Ring 16, D-35392 Giessen, Germany
³¹ Lanzhou University, Lanzhou 730000, People's Republic of China
³² Liaoning Normal University, Dalian 116029, People's Republic of China
³³ Liaoning University, Shenyang 110036, People's Republic of China
³⁴ Nanjing Normal University, Nanjing 210023, People's Republic of China
³⁵ Nanjing University, Nanjing 210093, People's Republic of China
³⁶ Nankai University, Tianjin 300071, People's Republic of China
³⁷ National Centre for Nuclear Research, Warsaw 02-093, Poland
³⁸ North China Electric Power University, Beijing 102206, People's Republic of China
³⁹ Peking University, Beijing 100871, People's Republic of China
⁴⁰ Qufu Normal University, Qufu 273165, People's Republic of China
⁴¹ Shandong Normal University, Jinan 250014, People's Republic of China
⁴² Shandong University, Jinan 250100, People's Republic of China
⁴³ Shanghai Jiao Tong University, Shanghai 200240, People's Republic of China
⁴⁴ Shanxi Normal University, Linfen 041004, People's Republic of China
⁴⁵ Shanxi University, Taiyuan 030006, People's Republic of China
⁴⁶ Sichuan University, Chengdu 610064, People's Republic of China
⁴⁷ Soochow University, Suzhou 215006, People's Republic of China
⁴⁸ South China Normal University, Guangzhou 510006, People's Republic of China
⁴⁹ Southeast University, Nanjing 211100, People's Republic of China
⁵⁰ State Key Laboratory of Particle Detection and Electronics, Beijing 100049, Hefei 230026, People's Republic of China
⁵¹ Sun Yat-Sen University, Guangzhou 510275, People's Republic of China
⁵² Suranaree University of Technology, University Avenue 111, Nakhon Ratchasima 30000, Thailand
⁵³ Tsinghua University, Beijing 100084, People's Republic of China
⁵⁴ Turkish Accelerator Center Particle Factory Group, (A)Istanbul University, 34010, Istanbul, Turkey; (B)Near East University, Nicosia, North Cyprus, Mersin 10, Turkey
⁵⁵ University of Chinese Academy of Sciences, Beijing 100049, People's Republic of China
⁵⁶ University of Groningen, NL-9747 AA Groningen, The Netherlands
⁵⁷ University of Hawaii, Honolulu, Hawaii 96822, USA
⁵⁸ University of Jinan, Jinan 250022, People's Republic of China
⁵⁹ University of Manchester, Oxford Road, Manchester, M13 9PL, United Kingdom
⁶⁰ University of Minnesota, Minneapolis, Minnesota 55455, USA
⁶¹ University of Muenster, Wilhelm-Klemm-Str. 9, 48149 Muenster, Germany
⁶² University of Oxford, Keble Rd, Oxford, UK OX13RH
⁶³ University of Science and Technology Liaoning, Anshan 114051, People's Republic of China

⁶⁴ University of Science and Technology of China, Hefei 230026, People's Republic of China

⁶⁵ University of South China, Hengyang 421001, People's Republic of China

⁶⁶ University of the Punjab, Lahore-54590, Pakistan

⁶⁷ University of Turin and INFN, (A)University of Turin, I-10125, Turin, Italy; (B)University of Eastern Piedmont, I-15121, Alessandria, Italy; (C)INFN, I-10125, Turin, Italy

⁶⁸ Uppsala University, Box 516, SE-75120 Uppsala, Sweden

⁶⁹ Wuhan University, Wuhan 430072, People's Republic of China

⁷⁰ Xinyang Normal University, Xinyang 464000, People's Republic of China

⁷¹ Yunnan University, Kunming 650500, People's Republic of China

⁷² Zhejiang University, Hangzhou 310027, People's Republic of China

⁷³ Zhengzhou University, Zhengzhou 450001, People's Republic of China

^a Also at the Moscow Institute of Physics and Technology, Moscow 141700, Russia

^b Also at the Novosibirsk State University, Novosibirsk, 630090, Russia

^c Also at the NRC "Kurchatov Institute", PNPI, 188300, Gatchina, Russia

^d Also at Goethe University Frankfurt, 60323 Frankfurt am Main, Germany

^e Also at Key Laboratory for Particle Physics, Astrophysics and Cosmology, Ministry of Education; Shanghai Key Laboratory for Particle Physics and Cosmology; Institute of Nuclear and Particle Physics, Shanghai 200240, People's Republic of China

^f Also at Key Laboratory of Nuclear Physics and Ion-beam Application (MOE) and Institute of Modern Physics, Fudan University, Shanghai 200443, People's Republic of China

^g Also at State Key Laboratory of Nuclear Physics and Technology, Peking University, Beijing 100871, People's Republic of China
^h Also at School of Physics and Electronics, Hunan University, Changsha 410082, China

ⁱ Also at Guangdong Provincial Key Laboratory of Nuclear Science, Institute of Quantum Matter, South China Normal University, Guangzhou 510006, China

^j Also at Frontiers Science Center for Rare Isotopes, Lanzhou University, Lanzhou 730000, People's Republic of China

^k Also at Lanzhou Center for Theoretical Physics, Lanzhou University, Lanzhou 730000, People's Republic of China

^l Also at the Department of Mathematical Sciences, IBA, Karachi, Pakistan

(Dated: November 23, 2022)

Using a sample of $(448.1 \pm 2.9) \times 10^6$ $\psi(3686)$ decays collected with the BESIII detector at BEPCII, we report an observation of Ξ^- transverse polarization with a significance of 7.3σ in the decay $\psi(3686) \rightarrow \Xi^-\bar{\Xi}^+$ ($\Xi^- \rightarrow \Lambda\pi^-$, $\bar{\Xi}^+ \rightarrow \bar{\Lambda}\pi^+$, $\Lambda \rightarrow p\pi^-$, $\bar{\Lambda} \rightarrow \bar{p}\pi^+$). The relative phase of the electric and magnetic form factors is determined to be $\Delta\Phi = (0.667 \pm 0.111 \pm 0.058)$ rad. This is the first measurement of the relative phase for a $\psi(3686)$ decay into a pair of $\Xi^-\bar{\Xi}^+$ hyperons. The Ξ^- decay parameters (α_{Ξ^-} , ϕ_{Ξ^-}) and their conjugates (α_{Ξ^+} , ϕ_{Ξ^+}), the angular-distribution parameter α_ψ , and the strong-phase difference $\delta_p - \delta_s$ for $\Lambda\pi^-$ scattering are measured to be consistent with previous BESIII results.

Charmonium decays into hyperon and antihyperon pair offer a clean laboratory to explore hyperon properties, such as their polarization and decay parameters, and to perform tests of fundamental symmetries. Taking advantage of the large J/ψ and $\psi(3686)$ data samples and the excellent performance of the detector, BESIII has reported a series of observations of hyperon polarization in charmonium decays, such as $J/\psi \rightarrow \Lambda\bar{\Lambda}$ [1] and $J/\psi, \psi(3686) \rightarrow \Sigma^+\bar{\Sigma}^-$ [2]. This has led to a renewed interest in both theoretical and experimental investigations in hyperon physics. Baryon-spin polarization in a vector-charmonium decay into a baryon-antibaryon pair was first considered in Ref. [3]. Such an effect requires that the decay amplitudes are complex and have nontrivial relative phase $\Delta\Phi$. To observe the baryon polarization some of the spin projections of the initial charmonium state must have different weights. This is possible if the state is produced in electron-positron annihilation with unpolarized beams since the photon, and therefore the charmonium, can only have ± 1 helicities. A comparison of the polarization found in J/ψ and $\psi(3686)$ decays may elucidate other puzzles in vector charmonia decays, such as breaking of the ‘12% rule’, which predicts that the ratio of branching fractions of $\psi(3686)$ and J/ψ decays into the same final state is 12% [4]. Experimentally,

only one such polarization comparison has been performed, using the $J/\psi, \psi(3686) \rightarrow \Sigma^+\bar{\Sigma}^-$ reactions [2]. The result reported in Ref. [2] is striking since the relative phase between the form factors has opposite sign and different absolute values $\Delta\Phi_{J/\psi} = -0.270(12)$ rad and $\Delta\Phi_{\psi(3686)} = 0.379(70)$ rad. Currently, there is no explanation for this behavior. To improve understanding, measurements for other baryon-antibaryon pairs are needed.

A natural extension of these hyperon-polarization measurements is to investigate Ξ^- decays in $J/\psi, \psi(3686) \rightarrow \Xi^-\bar{\Xi}^+$, where the measurement of the polarization of the Ξ^- hyperon is accessible via the process $\Xi^- \rightarrow \Lambda\pi^-$. The inclusion of charge-conjugate processes is implied throughout unless stated otherwise. The initial Ξ transverse polarization with respect to the scattering plane, \mathbf{P}_Ξ , is related to the child Λ polarization, \mathbf{P}_Λ , via the relation [5],

$$\mathbf{P}_\Lambda = \alpha_{\Xi^-}\hat{\mathbf{z}}_\Xi + \beta_{\Xi^-}\mathbf{P}_\Xi \times \hat{\mathbf{z}}_\Xi + \gamma_{\Xi^-}\hat{\mathbf{z}}_\Xi \times (\mathbf{P}_\Xi \times \hat{\mathbf{z}}_\Xi), \quad (1)$$

where $\hat{\mathbf{z}}_\Xi$ is the unit vector defined in Fig. 1 and α_{Ξ^-} , β_{Ξ^-} , and γ_{Ξ^-} are the asymmetry decay parameters for the $\Xi^- \rightarrow \Lambda\pi^-$ decay. The decay parameters β_{Ξ^-} and γ_{Ξ^-} are related and can be represented by a single parameter $\phi_{\Xi^-} =$

$\tan^{-1}(\beta_{\Xi^-}/\gamma_{\Xi^-})$. The joint angular distribution describes

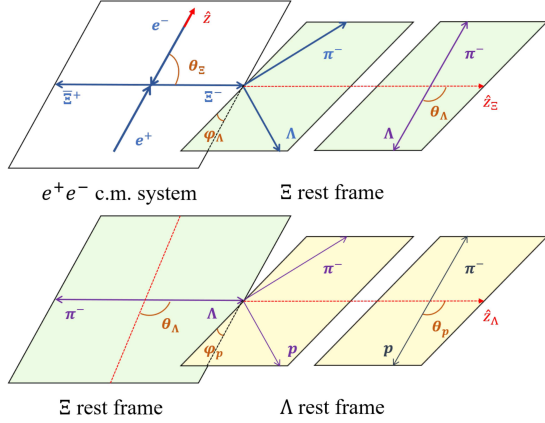


FIG. 1. The definition of the helicity angles in different rest frames. The angles θ_{Ξ} , θ_{Λ} , ϕ_{Λ} , θ_p , φ_p are the polar and azimuthal helicity angles of the Ξ , Λ hyperons and the proton in three reference frames: e^+e^- center-of-mass (c.m.) system, Ξ rest frame and Λ rest frame, respectively. In the e^+e^- c.m. system, the \hat{z} axis is along the e^+ momentum direction, the \hat{z}_{Ξ} is along the Ξ^- momentum direction. In the Ξ rest frame, the polar axis direction is \hat{z}_{Ξ} , \hat{y}_{Ξ} is along $\hat{z} \times \hat{z}_{\Xi}$ and \hat{z}_{Λ} is along the Λ momentum direction. In the Λ rest frame, the polar axis direction is \hat{z}_{Λ} and \hat{y}_{Λ} is along $\hat{z}_{\Xi} \times \hat{z}_{\Lambda}$. The vector $\mathbf{P}_{\Xi} \times \hat{z}_{\Lambda}$ is along the \hat{y}_{Λ} axis.

the spin correlation and polarization, which is expressed as [6]

$$\begin{aligned} \mathcal{W}(\xi; \Omega) &= \sum_{\mu, \bar{\nu}=0}^3 C_{\mu\bar{\nu}}(\theta_{\Xi}; \alpha_{\psi}, \Delta\Phi) \sum_{\mu'=0}^3 \sum_{\nu'=0}^3 a_{\mu\mu'}^{\Xi^-} a_{\mu'0}^{\Lambda} a_{\nu\nu'}^{\Xi^+} a_{\nu'0}^{\bar{\Lambda}}. \end{aligned} \quad (2)$$

In Eq. (2), $\Omega = (\alpha_{\psi}, \Delta\Phi, \alpha_{\Lambda}, \alpha_{\bar{\Lambda}}, \alpha_{\Xi^-}, \alpha_{\Xi^+}, \phi_{\Xi^-}, \phi_{\Xi^+})$ represent the production and decay parameters, the kinematic variables $\xi = (\theta_{\Xi}, \theta_{\Lambda}, \phi_{\Lambda}, \theta_{\bar{\Lambda}}, \phi_{\bar{\Lambda}}, \theta_p, \varphi_p, \theta_{\bar{p}}, \varphi_{\bar{p}})$ describe the production and the multistep decays, the spin density matrix $C_{\mu\bar{\nu}}$ describes the spin configuration of the entangled hyperon-antihyperon pairs, and $a_{\mu\nu}^H$ is the propagation of the spin-density matrix based on the corresponding helicity variables and decay parameters.

Equation (2) characterizes the Ξ^- polarization and spin correlation via the angular-distribution parameter α_{ψ} and $\Delta\Phi$. The free parameters (Ω) are determined by a fit of the function defined in Eq. (2) to the data. If $\Delta\Phi$ is nonzero, it indicates a nonzero polarization of Ξ^- , and all other parameters can be determined simultaneously.

Recently BESIII observed Ξ^- polarization in $J/\psi \rightarrow \Xi^-\bar{\Xi}^+$ decays [7] for the first time and the process was used for novel CP symmetry tests by measuring the observables $A_{CP,\Xi} = (\alpha_{\Xi^-} + \alpha_{\Xi^+})/(\alpha_{\Xi^-} - \alpha_{\Xi^+})$ and $\Delta\phi_{CP} = (\phi_{\Xi^-} + \phi_{\Xi^+})/2$. CP -violation tests performed with the $\psi(3686) \rightarrow \Xi^-\bar{\Xi}^+$ data set have lower precision than those made in J/ψ decays, but the sample can also be exploited for an independent measurement of the strong phase difference, $\delta_p - \delta_s$,

for $\Lambda\pi^-$ scattering, where subscript $p(s)$ denotes P(S)-wave. This quantity determines the sensitivity of the $A_{CP,\Xi}$ variable to the CP -violating phase difference $\xi_p - \xi_s$ in the decay. A nonzero value of $\delta_p - \delta_s$ is necessary to observe CP violation via the $A_{CP,\Xi}$ variable. It can be determined via the formula $\tan(\delta_p - \delta_s) = \langle \beta_{\Xi} \rangle / \langle \alpha_{\Xi} \rangle$. The value of $\langle \beta_{\Xi} \rangle$ is determined from the averages of decay parameters $\langle \alpha_{\Xi} \rangle$ and $\langle \phi_{\Xi} \rangle$. We make these calculations of averages with method used in the particle data group (PDG) and take the same sign as decay parameters of Ξ^- hyperon. At present there is a tension between the $\phi_{\Xi^-} = -0.042 \pm 0.016$ rad determined from the HyperCP [8] experiment and the BESIII value for $\langle \phi_{\Xi} \rangle = 0.016 \pm 0.014 \pm 0.007$ rad [7]. This tension causes the difference of $\delta_p - \delta_s$ over one standard deviation in these two measurements, $\delta_p - \delta_s = (8.0 \pm 5.0) \times 10^{-2}$ rad for HyperCP [8] and $\delta_p - \delta_s = (-4.0 \pm 3.3 \pm 1.7) \times 10^{-2}$ rad for BESIII experiment [7]. A model-dependent prediction of CP violation within the context of the Standard Model (SM) gives $A_{CP,\Xi} \sim -7 \times 10^{-5}$ [9], and heavy-baryon perturbation theory predicts the strong-phase difference $\delta_p - \delta_s = (1.9 \pm 4.9) \times 10^{-2}$ rad [10].

In this paper we present an analysis of the angular distributions of the Ξ^- hyperon and its final-state particles in the decay $\psi(3686) \rightarrow \Xi^-\bar{\Xi}^+$, and subsequent $\Xi^- \rightarrow \Lambda\pi^-$ and $\Lambda \rightarrow p\pi^-$ decays, using a sample of 448.1×10^6 $\psi(3686)$ events [11] collected with the BESIII detector [12]. In addition to measuring the spin polarization and decay asymmetry parameters of the $\Xi^-(\bar{\Xi}^+)$ hyperon, the CP observables $A_{CP,\Xi}$ and $\Delta\phi_{CP}$ are also determined.

Candidates for $\psi(3686) \rightarrow \Xi^-\bar{\Xi}^+$ events are selected using a full reconstruction of the subsequent decays $\Xi^- \rightarrow \Lambda\pi^-$, $\Lambda \rightarrow p\pi^-$. To study the decay parameters for the $\psi(3686) \rightarrow \Xi^-\bar{\Xi}^+$ decay, five million Monte Carlo (MC) simulation events with $\psi(3686) \rightarrow \Xi^-\bar{\Xi}^+ \rightarrow \pi^-\pi^+\Lambda\bar{\Lambda} \rightarrow p\bar{p}\pi^-\pi^-\pi^+\pi^+$ are generated according to a uniform distribution using the KKMC generator [13, 14]. To study the potential background contributions, an inclusive MC sample of 350 million $\psi(3686)$ decays is used, where the production of the $\psi(3686)$ resonance is simulated with the KKMC generator, the subsequent decays are processed via EVTGEN [15, 16] according to the measured branching fractions provided by the PDG [17], and the remaining unmeasured decay modes are generated with LUNDCHARM [18, 19].

Charged tracks are required to be reconstructed in the main drift chamber within its angular coverage $|\cos\theta| < 0.93$, where θ is the polar angle with respect to the positron beam direction. Particle identification (PID) of the protons and pions is performed by considering the track momentum. Tracks with momentum above (below) 0.5 GeV/c are assigned the proton (pion) hypothesis. Events with at least two π^- , two π^+ , one proton and one antiproton are retained for further analysis.

To reconstruct Λ candidates, a secondary vertex fit [20] is applied to all $p\pi^-$ combinations. When there is more

than one combination, the one with the minimum value of $\sqrt{(M_{p\pi^-} - m_\Lambda)^2 + (M_{\bar{p}\pi^+} - m_{\bar{\Lambda}})^2}$ among all $p\pi^-$ combinations is chosen, where $M_{p\pi^-}$ is the invariant mass of the $p\pi^-$ pair and m_Λ is the known mass of the Λ baryon [17]. The $p\pi^-$ invariant mass of the selected candidate is required to be within $5 \text{ MeV}/c^2$ of the known Λ mass. This criterion is optimized by the $S/\sqrt{S+B}$ figure of merit (FOM) using MC simulation, where S is the number of signal MC events and B is the number of expected background events obtained from the simulation. To further suppress backgrounds from non- Λ events, the Λ decay length, *i.e.* the distance between its production and decay positions, is required to be greater than zero. The Ξ^- candidates are reconstructed with a similar strategy using a secondary vertex fit and the candidate with the minimum value of $\sqrt{(M_{\Lambda\pi^-} - m_\Xi)^2 + (M_{\bar{\Lambda}\pi^+} - m_{\Xi})^2}$ from all $\Lambda\pi^-$ combinations is selected. Here, $M_{\Lambda\pi^-}$ is the invariant mass of the $\Lambda\pi^-$ pair and m_Ξ is the known mass of the Ξ^- hyperon [17]. Furthermore, the Ξ^- decay length is required to be greater than zero.

To further suppress backgrounds and improve the mass resolution, a four-constraint (4C) kinematic fit, imposing energy-momentum conservation from the initial e^+e^- to the final $\Xi^-\bar{\Xi}^+$ state, is applied for all $\Xi^-\bar{\Xi}^+$ hypotheses after the full reconstruction. Events with $\chi^2_{4C} < 200$ are retained based on the FOM optimization. Figure 2 shows the two-dimensional distribution of $M_{\Lambda\pi^-}$ versus $M_{\bar{\Lambda}\pi^+}$ after performing the 4C kinematic fit. A clear enhancement around the known Ξ^- mass can be seen. The $\Lambda\pi^-$ invariant mass is required to be within $8 \text{ MeV}/c^2$ of the known Ξ^- mass, which is determined through the FOM. The signal region shown in Fig. 2 is marked by S . After applying the above event selection criteria to the data, detailed event type analysis of the inclusive $\psi(3686)$ MC sample [21] shows that the remaining backgrounds in this analysis are mainly from non- Ξ^- events, such as $e^+e^- \rightarrow \pi^+\pi^-\Lambda\bar{\Lambda}$. The background level is estimated using the sideband method. We take four sideband regions and make a scaling of the backgrounds to the signal region, *i.e.*, $\sum_{j=1}^4 B_j / 4$, where j denotes one of the four regions shown in Fig. 2, and B_j is the yield in that region. The upper and lower sideband regions are defined as $1.338 \text{ GeV}/c^2 < M_{\Lambda\pi^-} < 1.354 \text{ GeV}/c^2$ and $1.290 \text{ GeV}/c^2 < M_{\Lambda\pi^-} < 1.306 \text{ GeV}/c^2$ respectively, which means that the sideband region is about $[6\sigma, 12\sigma]$ away from the signal peak position. A total of 5358 signal events survive the above selection criteria. A scaled background of 15 ± 4 events is estimated with the sideband method. A similar number of background events (15 ± 4) is estimated to be present from $e^+e^- \rightarrow \Xi^-\bar{\Xi}^+$ continuum production. This is deduced by applying the event selection to 2.9 fb^{-1} of data collected at a collision energy of $3.773 \text{ GeV}/c^2$ [22, 23]. In total therefore, the background level is determined to be 0.6%, which can be considered negligible for the analysis.

An unbinned maximum-likelihood (MLL) fit is performed to determine the Ξ^- spin-polarization parameters. Based on a previous study [1], we present CP conservation in Λ decays under the current statistics; thus, we assume CP conservation

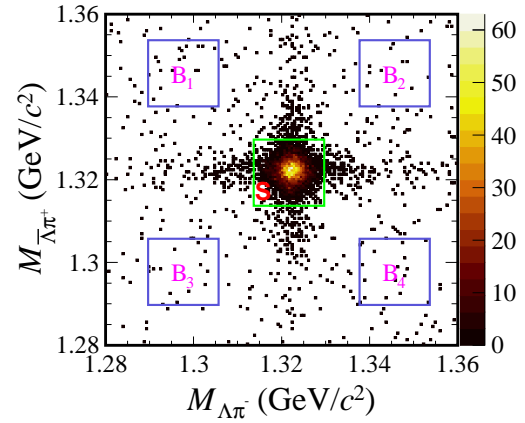


FIG. 2. Distribution of $M_{\Lambda\pi^-}$ versus $M_{\bar{\Lambda}\pi^+}$. The box marked by S shows the signal region, the boxes marked by B_j ($j = 1, 2, 3, 4$) denote the sideband regions.

of Λ and fix the decay parameters $\alpha_{\Lambda/\bar{\Lambda}}$ to the average value $(\alpha_\Lambda - \alpha_{\bar{\Lambda}})/2$ [1] in the fit. This assumption would not affect the CP tests in Ξ decays under the current statistics. The joint likelihood function is

$$\mathcal{L} = \prod_{i=1}^N \mathcal{P}(\xi_i; \Omega) = \prod_{i=1}^N \frac{\mathcal{W}(\xi_i; \Omega)\epsilon(\xi_i)}{\mathcal{N}(\Omega)}, \quad (3)$$

where \mathcal{P} is the probability to produce event i based on the measured parameters ξ_i and the set of observables Ω , N is the number of data events after all selection criteria, \mathcal{W} is defined in Eq. (2), $\epsilon(\xi_i)$ is the detection efficiency and the normalization factor $\mathcal{N}(\Omega) = \int \mathcal{W}(\xi; \Omega)\epsilon(\xi)d\xi$. The negative value of the logarithm of \mathcal{L} is minimized by using the MINUIT software package [24]. The default fit contains no background term, as there is negligible contamination in the final sample. However, background is considered as a source of systematic uncertainty.

The results of the fit are given in Table I. The relative phase $\Delta\Phi$ for $\psi(3686) \rightarrow \Xi^-\bar{\Xi}^+$ decay is measured for the first time and differs from zero. The decay-asymmetry parameters α_{Ξ^-} and α_{Ξ^+} agree within their statistical uncertainties but are somewhat lower than the PDG average value ($\alpha_{\Xi^-} = -0.401 \pm 0.010$) [17]. The strong-phase difference, $\delta_p - \delta_s$, is consistent with the BESIII result measured from the $J/\psi \rightarrow \Xi^-\bar{\Xi}^+$ decay [7], and lies around two standard deviations below the HyperCP measurement [8]. The other parameters are compatible with earlier measurements.

The transverse Ξ^- polarization, P_y , is given by

$$P_y = \sqrt{1 - \alpha_\psi^2} \sin \theta_\Xi \cos \theta_\Xi \sin \Delta\Phi / (1 + \alpha_\psi \cos^2 \theta_\Xi) \quad (4)$$

and the spin correlations C_{ij} ($i, j = x, y, z$), are related to the $C_{\mu\nu}$ in Eq. (2) as follows

TABLE I. The numerical results for the measurements of the Ξ^- polarization and the decay parameters. Also shown are the analogous parameters for the $J/\psi \rightarrow \Xi^-\bar{\Xi}^+$ decay as reported in Ref. [7]. The first uncertainty is statistical and the second systematic.

Parameter	$\psi(3686) \rightarrow \Xi^-\Xi^+$	$J/\psi \rightarrow \Xi^-\Xi^+$
α_ψ	$0.693 \pm 0.048 \pm 0.049$	$0.586 \pm 0.012 \pm 0.010$
$\Delta\Phi$ (rad)	$0.667 \pm 0.111 \pm 0.058$	$1.213 \pm 0.046 \pm 0.016$
α_{Ξ^-}	$-0.344 \pm 0.025 \pm 0.007$	$-0.376 \pm 0.007 \pm 0.003$
α_{Ξ^+}	$0.355 \pm 0.025 \pm 0.002$	$0.371 \pm 0.007 \pm 0.002$
ϕ_{Ξ^-} (rad)	$0.023 \pm 0.074 \pm 0.003$	$0.011 \pm 0.019 \pm 0.009$
ϕ_{Ξ^+} (rad)	$-0.123 \pm 0.073 \pm 0.004$	$-0.021 \pm 0.019 \pm 0.007$
$\delta_p - \delta_s$ ($\times 10^{-1}$ rad)	$-2.0 \pm 1.3 \pm 0.1$	$-0.40 \pm 0.33 \pm 0.17$
$A_{CP,\Xi}$ ($\times 10^{-2}$)	$-1.5 \pm 5.1 \pm 1.0$	$0.60 \pm 1.34 \pm 0.56$
$\Delta\phi_{CP}$ ($\times 10^{-2}$ rad)	$-5.0 \pm 5.2 \pm 0.3$	$-0.48 \pm 1.37 \pm 0.29$

$$C_{\mu\bar{\nu}} = (1 + \alpha_\psi \cos^2 \theta_\Xi) \begin{pmatrix} 1 & 0 & P_y & 0 \\ 0 & C_{xx} & 0 & C_{xz} \\ -P_y & 0 & C_{yy} & 0 \\ 0 & -C_{xz} & 0 & C_{zz} \end{pmatrix}. \quad (5)$$

Figure 3 shows the resulting P_y polarization and spin correlations together with the fit results. The P_y polarization and the spin correlations are clearly nonzero.

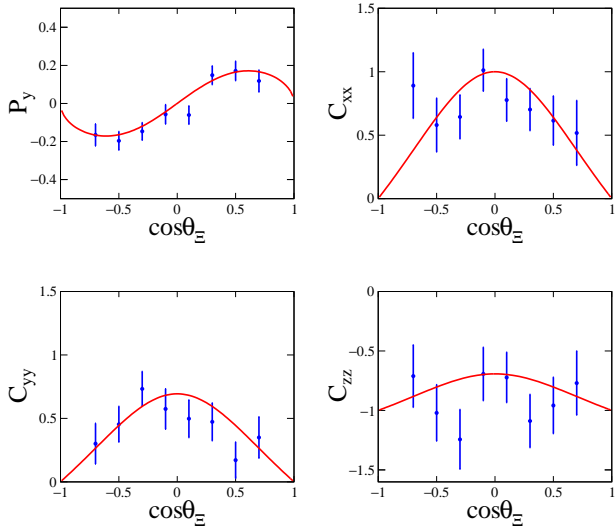


FIG. 3. Polarization P_y and spin correlations C_{xx} , C_{yy} and C_{zz} in $\psi(3686) \rightarrow \Xi^-\bar{\Xi}^+$ as a function of $\cos \theta_\Xi$. The dots with error bars are the binned experimental result and the red lines give the result of the global MLL fit. The error bar represents the statistical uncertainty.

Possible sources of systematic bias on the parameter measurements are considered. They include the fit method, the Ξ^- reconstruction, the 4C kinematic fit, the background and the decay parameters for $\Lambda \rightarrow p\pi$. We validate the reliability of the fit results by an input and output check based on 100 pseudodata samples. The helicity amplitude formula is based on Eq. (2) and the measured polarization parameters in this work are used as the input parameters, where the central values used in the generation of the number of events for each

pseudodata sample are the same as measured in the data sample. The average difference between input and the output result is taken as the systematic uncertainty. The systematic uncertainty due to the Ξ^- hyperon reconstruction incorporates the track selection, PID criteria, requirements on mass window and decay length of $\Xi^-(\Lambda)$, and is studied with a control sample of $\psi(3686) \rightarrow \Xi^-\bar{\Xi}^+$ decays using the same method as in Refs. [25–33]. From this we obtain the efficiency difference between the data and MC event reconstruction. Then we apply a correction to the MC simulation with the efficiency difference described above, and repeat the fit. The differences between the new values and the nominal values are taken as the systematic uncertainties of the parameters resulting from the Ξ^- reconstruction. The systematic uncertainty due to the 4C kinematic fit is studied by correcting the helical-track parameters for each charged particle. For the nominal result, we take the uncorrected results. We repeat the full fit procedure using a MC sample with the track correction and take the difference between the two fit results as a systematic uncertainty. To assign a systematic uncertainty from background, which is not included in the nominal fit, we repeat the fit taking in consideration the backgrounds from the sideband region and continuum process in the log-likelihood function. The differences between the new values and the nominal values are taken as the systematic uncertainties of the parameters resulting from backgrounds. The uncertainty from the decay parameters $\alpha_{\Lambda/\bar{\Lambda}}$ of $\Lambda \rightarrow p\pi^-/\bar{\Lambda} \rightarrow \bar{p}\pi^+$ is estimated by varying the nominal value, obtained by the average in Ref. [1], by $\pm 1\sigma$. The largest difference in the results is taken as the systematic uncertainty. Assuming all sources are independent, the total systematic uncertainty is determined by taking the square root of their the quadratic sum and the results are given in Table II.

In summary, we report an observation of the Ξ^- hyperon spin polarization in the process $e^+e^- \rightarrow \psi(3686) \rightarrow \Xi^-\bar{\Xi}^+$. The measured parameters are summarized in Table I. The relative phase between the electric and magnetic psionic form factors, $\Delta\Phi$, in the $\psi(3686) \rightarrow \Xi^-\bar{\Xi}^+$ decay is determined to be different from zero for the first time with a significance of 7.3σ , including the systematic uncertainty, by comparing the most conservative differences of likelihoods of the base-

TABLE II. The absolute systematic uncertainties on the fit parameters. (Entries of 0.000 indicate a contribution less than 0.001.)

Source	α_ψ	$\Delta\Phi$	α_{Ξ^-}	$\alpha_{\bar{\Xi}^+}$	ϕ_{Ξ^-}	$\phi_{\bar{\Xi}^+}$
Fit method	0.001	0.026	0.006	0.000	0.002	0.001
Ξ^- reconstruction	0.027	0.027	0.000	0.000	0.001	0.000
$\bar{\Xi}^+$ reconstruction	0.040	0.042	0.001	0.000	0.001	0.000
4C kinematic fit	0.002	0.004	0.002	0.001	0.002	0.004
Sideband	0.004	0.004	0.000	0.000	0.000	0.000
Continuum process	0.002	0.001	0.000	0.000	0.000	0.000
Λ -decay parameter	0.006	0.011	0.001	0.002	0.000	0.000
Total	0.049	0.058	0.007	0.002	0.003	0.004

line fit and the one assuming no polarization. This result differs significantly from the corresponding relative phase in the J/ψ decay [7]. The behavior is also noticeably different to that seen in decays of charmonia to Σ baryons, where the corresponding phase is negative and around four times smaller in magnitude than for Ξ baryons in J/ψ decays, and around two times smaller in the case of $\psi(3686)$ decays [2]. The results provide important input for understanding the difference of the α_ψ , $\Delta\Phi$ values at different energies and different charmonia states, and even insight into double-strange versus single-strange hyperon pair production [34, 35]. Further input from the theory community and new measurements in related decay modes are needed to interpret these results. Other decay parameters (α_{Ξ^-} , $\alpha_{\bar{\Xi}^+}$, ϕ_{Ξ^-} , $\phi_{\bar{\Xi}^+}$) for $\Xi^- \rightarrow \Lambda\pi^-$ and $\bar{\Xi}^+ \rightarrow \bar{\Lambda}\pi^+$ decays including the angular distribution parameters (α_ψ) are measured to be consistent with previous publications within their uncertainties [7, 26]. The measurement of the strong phase difference, $\delta_p - \delta_s$, constitutes an independent determination of this important quantity describing the strong interaction between the Λ and π^- hadrons. The result is consistent with the heavy-baryon perturbation theory [10] and agrees with the recent BESIII measurement performed with J/ψ decays [7], and is around two standard deviations lower than the HyperCP measurement of this parameter [8]. The CP observables $A_{CP,\Xi}$ and $\Delta\phi_{CP}$ are determined from the measurements of the $\Xi^-(\bar{\Xi}^+)$ decay parameters. The results are consistent with the CP conservation hypothesis. Our measurement of $A_{CP,\Xi}$ is in agreement with the SM expectation.

ACKNOWLEDGMENTS

The BESIII Collaboration thanks the staff of BEPCII and the IHEP computing center for their strong support. This work is supported in part by National Key R&D Program of China under Contracts Nos. 2020YFA0406400, 2020YFA0406300; National Natural Science Foundation of China (NSFC) under Contracts Nos. 12075107, 11625523, 11635010, 11735014, 11822506, 11835012, 11905236, 11935015, 11935016, 11935018, 11961141012, 12047501, 12022510, 12025502, 12035009, 12035013, 12061131003 and 12225509; the Chinese Academy of Sciences (CAS) Large-Scale Scientific Fa-

cility Program; Joint Large-Scale Scientific Facility Funds of the NSFC and CAS under Contracts Nos. U1732263, U1832207; CAS Key Research Program of Frontier Sciences under Contract No. QYZDJ-SSW-SLH040; 100 Talents Program of CAS; Institute of Nuclear and Particle Physics, Astronomy and Cosmology (INPAC) and Shanghai Key Laboratory for Particle Physics and Cosmology; ERC under Contract No. 758462; European Union Horizon 2020 research and innovation programme under Contract No. Marie Skłodowska-Curie grant agreement No 894790; German Research Foundation DFG under Contracts Nos. 443159800, Collaborative Research Center CRC 1044, FOR 2359, GRK 2149; Istituto Nazionale di Fisica Nucleare, Italy; Ministry of Development of Turkey under Contract No. DPT2006K-120470; National Science and Technology fund; Olle Engkvist Foundation under Contract No. 200-0605; Lundström-Åmans Foundation; STFC (United Kingdom); The Knut and Alice Wallenberg Foundation (Sweden) under Contract No. 2016.0157; The Royal Society, (United Kingdom) under Contracts Nos. DH140054, DH160214; The Swedish Research Council; Polish National Science Centre under Contract No. 2019/35/O/ST2/02907; U. S. Department of Energy under Contracts Nos. DE-FG02-05ER41374, DE-SC-0012069.

-
- [1] M. Ablikim *et al.* (BESIII Collaboration), *Nat. Phys.* **15**, 631 (2019).
 - [2] M. Ablikim *et al.* (BESIII Collaboration), *Phys. Rev. Lett.* **125**, 052004 (2020).
 - [3] G. Fäldt and A. Kupsc, *Phys. Lett. B* **772**, 16 (2017).
 - [4] T. Appelquist and H. D. Politzer, *Phys. Rev. Lett.* **34**, 43 (1975).
 - [5] T. D. Lee and C. N. Yang, *Phys. Rev.* **108**, 1645 (1957).
 - [6] E. Perotti, G. Fäldt, A. Kupsc, S. Leupold, and J. J. Song, *Phys. Rev. D* **99**, 056008 (2019).
 - [7] M. Ablikim *et al.* (BESIII Collaboration), *Nature (London)* **606**, 64 (2022).
 - [8] M. Huang *et al.* (HyperCP Collaboration), *Phys. Rev. Lett.* **93**, 011802 (2004).
 - [9] J. F. Donoghue, X. G. He, and S. Pakvasa, *Phys. Rev. D* **34**, 833 (1986).
 - [10] J. Tandean and G. Valencia, *Phys. Rev. D* **67**, 056001 (2003).
 - [11] M. Ablikim *et al.* (BESIII Collaboration), *Chin. Phys. C* **42**, 023001 (2018).

- [12] M. Ablikim *et al.* (BESIII Collaboration), *Nucl. Instrum. Methods Phys. Res., Sect. A* **614**, 345 (2010).
- [13] S. Jadach, B. F. L. Ward, and Z. Was, *Comput. Phys. Commun.* **130**, 260 (2000).
- [14] S. Jadach, B. F. L. Ward, and Z. Was, *Phys. Rev. D* **63**, 113009 (2001).
- [15] R. G. Ping, *Chin. Phys. C* **32**, 599 (2008).
- [16] D. J. Lange, *Nucl. Instrum. Methods Phys. Res., Sect. A* **462**, 152 (2001).
- [17] P. A. Zyla *et al.* (Particle Data Group), *Prog. Theor. Exp. Phys.* **2020**, 083C01 (2020).
- [18] J. C. Chen, G. S. Huang, X. R. Qi, D. H. Zhang, and Y. S. Zhu, *Phys. Rev. D* **62**, 034003 (2000).
- [19] R. L. Yang, R. G. Ping, and H. Chen, *Chin. Phys. Lett.* **31** 061301 (2014).
- [20] M. Xu, K. L. He, Z. P. Zhang, Y. F. Wang, J. M. Bian, G. F. Cao, X. X. Cao, S. J. Chen, Z. Y. Deng, C. D. Fu *et al.*, *Chin. Phys. C* **33**, 428 (2009).
- [21] X. Y. Zhou, S. X. Du, G. Li, and C. P. Shen, *Comput. Phys. Commun.* **258**, 107540 (2021).
- [22] M. Ablikim *et al.* (BESIII Collaboration), *Chin. Phys. C* **37**, 123001 (2013).
- [23] M. Ablikim *et al.* (BESIII Collaboration), *Phys. Lett. B* **753**, 629 (2016).
- [24] F. James and M. Roos, *Comput. Phys. Commun.* **10**, 343 (1975).
- [25] M. Ablikim *et al.* (BESIII Collaboration), *Phys. Rev. D* **87**, 032007 (2013).
- [26] M. Ablikim *et al.* (BESIII Collaboration), *Phys. Rev. D* **93**, 072003 (2016).
- [27] M. Ablikim *et al.* (BESIII Collaboration), *Phys. Lett. B* **770**, 217 (2017).
- [28] M. Ablikim *et al.* (BESIII Collaboration), *Phys. Rev. D* **100**, 051101 (2019).
- [29] M. Ablikim *et al.* (BESIII Collaboration), *Phys. Rev. Lett.* **124**, 032002 (2020).
- [30] M. Ablikim *et al.* (BESIII Collaboration), *Phys. Rev. D* **104**, L091104 (2021).
- [31] M. Ablikim *et al.* (BESIII Collaboration), *Phys. Rev. D* **103**, 012005 (2021).
- [32] M. Ablikim *et al.* (BESIII Collaboration), *Phys. Lett. B* **820**, 136557 (2021).
- [33] M. Ablikim *et al.* (BESIII Collaboration), *Phys. Rev. D* **105**, L011101 (2022).
- [34] R. B. Ferroli, A. Mangoni, S. Pacetti, and K. Zhu, *Phys. Lett. B* **799**, 135041 (2019).
- [35] R. B. Ferroli, A. Mangoni, S. Pacetti, and K. Zhu, *Phys. Rev. D* **103**, 016005 (2021).